Inorganic Chemistry

Article

pubs.acs.org/IC

Octahedral Metal Clusters as Building Blocks of Trimetallic Superexpanded Prussian Blue Analogues

Jian-Jun Zhang[†] and Abdou Lachgar*[,‡,§]

[‡]Department of Chemistry, and [§]Center for Energy, Environment and Sustainability, Wake Forest University, Winston-Salem, North Carolina 27109, United States

[†]Department of Chemistry, Dalian University of Technology, Dalian 116024, P. R. China

Supporting Information

ABSTRACT: The self-assembly of octahedral metal clusters (diamagnetic $[Nb_6Cl_{12}(CN)_6]^{4-}$ or paramagnetic $[Ta_6Cl_{12}(CN)_6]^{3-}$), $[Mn(salen)]^+$ [salen = *N*,*N*′-ethylenebis(salicylidene)iminate] and mononuclear $\{M'(CN)_x\}$ polycyanometallates ($[Fe(CN)_6]^{4-}$, $[Cr(CN)_6]^{3-}$, $[Fe(CN)_5(NO)]^{2-}$, or $[Ni(CN)_4]^{2-}$) building blocks results in the formation of a series of six cluster-containing 3D heterotrimetallic frameworks: $[H_3O]_2[Nb_6Cl_{12}(CN)_6[Mn(salen)]_6Fe(CN)_6]\cdot 3H_2O$ (**1**), $[H_3O][Nb_6Cl_{12}(CN)_6[Mn(salen)]_6Cr(CN)_6]\cdot 4H_2O$ (**2**), $[Nb_6Cl_{12}(CN)_6[Mn(salen)]_6Fe(CN)_5(NO)]\cdot 5H_2O$ (**3**), $[Nb_6Cl_{12}(CN)_6[Mn(salen)]_6Ni(CN)_4]\cdot 7H_2O$ (**4**), $[H_3O]$-$[Ta_6Cl_{12}(CN)_6[Mn(salen)]_6Fe(CN)_6]\cdot 4H_2O$ (**5**), and $[Ta_6Cl_{12}(CN)_6[Mn(salen)]_6Cr(CN)_6]\cdot 7H_2O$ (**6**). Single-crystal X-ray diffraction analyses show that compounds **1**, **2**, **5**, and **6** have distorted face-centered-cubic frameworks that can be considered as superexpanded Prussian blue analogues built of two different hexacyanometallate nodes and expanded by insertion of the $[Mn(salen)]^+$ complex, while **4** features a quasi-superexpanded Prussian blue framework because the structure is based on the hexacyano metal cluster and disordered tetracyano $[Ni(CN)_4]^{2-}$ nodes. The powder X-ray diffraction of **3** indicates that it possesses a quasi-superexpanded Prussian blue framework based on the hexacyano cluster and disordered pentacyano $[Fe(CN)_5(NO)]^{2-}$ nodes. Compound **6** is the first compound containing three 3d−3d′−M_6 cluster (4d) spin centers. Magnetic measurements reveal that the overall magnetic nature can be systematically controlled by the choice of the octahedral metal cluster and polycyanometallate nodes. H_2/N_2 adsorption and thermal stability of the compounds were investigated.

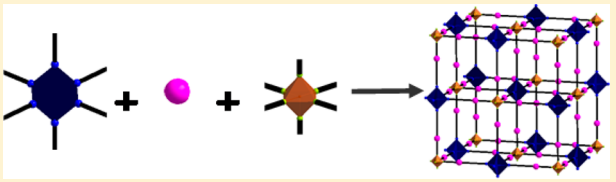

INTRODUCTION

The assembly of functional molecular building blocks into crystalline polymeric materials through coordination bonds or other weak interactions has many advantages over traditional stepwise syntheses and was demonstrated to be an effective approach to fabricating new materials.[1] Using this approach, numerous materials with fascinating structures and important properties have been prepared through the reactions of cyanometallate building blocks.[2] These compounds show novel functionalities due to strong interactions mediated by the linear cyanide bridges. The oldest and most interesting example is the Prussian blue framework, $Fe_4[Fe(CN)_6]_3\cdot 14H_2O$, and its analogues derived from the assembly of hexacyanometalate ions $[M(CN)_6]^{n-}$ and simple transition-metal ions. These compounds show interesting magnetic and other properties that can be affected through the judicious choice of building block components.[3]

Heterometallic complexes represent an important class of materials with interesting physicochemical properties resulting from electronic interactions between metal ions located in close proximity in one molecular system. They have attracted considerable attention owing to their potential use in catalysis,[4] mimicking the active sites of metal enzymes,[5] and molecular magnetism.[6] Heterobimetallic compounds were the first examples to be reported, followed by heterotrimetallic compounds, especially those containing three different spin carriers.[7,8] However, most heterotrimetallic compounds are based on discrete molecules, and extended frameworks are rare.[9] To the best of our knowledge, only two three-dimensional (3D) heterotrimetallic compounds have been reported.[9a,10] Two synthesis strategies have been developed for the rational preparation of heterotrimetallic compounds. The first strategy involves the preparation of a precursor metal complex containing two metal ions (a macrocyclic ligand is preferred), and then the complex precursor acts as a "ligand" toward a third metal ion.[9a] The second strategy is a "one-pot" method, which relies on the self-assembly of three suitable molecular building blocks containing three different metal ions.[10]

Metal clusters with strong metal−metal bonds represent one of the major contributions that John Corbett made to the field of chemistry.[11] They were indeed "its forte". Octahedral metal clusters can be classified into three different types depending on the nature of the metal atoms and inner ligands: $M_6L^i_8L^a_6$ clusters with 8 face-capped inner ligands; $M_6L^i_{12}L^a_6$ clusters

Special Issue: To Honor the Memory of Prof. John D. Corbett

Received: October 3, 2014
Published: January 15, 2015

DOI: 10.1021/ic502401n
Inorg. Chem. 2015, 54, 1082−1090

with 12 edge-capped inner ligands; $M_6ZL^i_8L^a_6$ or $M_6ZL^i_{12}L^a_6$ clusters with an interstitial atom located at the center of the metal cage.[12] These clusters are the main building units in the structure of Chevrel phases and are characterized by their single-metal-ion-like behavior, large size and interesting properties arising from the presence of metal−metal bonds, and diverse electronic structures. When functionalized with suitable ligands at the axial sites, these clusters can be used as bridging "ligands" for simple metal ions or coordinatively unsaturated metal complexes to form supramolecular assemblies or infinite extended networks with different dimensions.[13−16] For instance, the reaction between $\{Re_{6-n}Os_n\}$ clusters and copper(II) metal complexes led to the formation of a series of isolated cluster-based heterotrimetallic compounds, which show interesting magnetic exchange interactions between metal clusters and Cu^{2+} ions.[17] Also, several reports have shown that the replacement of $[Fe(CN)_6]^{4-}$ by octahedral metal cluster analogues $[Re_6X_8(CN)_6]^{n-}$ (X = chalcogenide) can give rise to a series of compounds that can be viewed as a direct expansion of Prussian blue, some of them with large cavities and interesting gas absorption properties.[18]

In our quest to introduce functionality into Prussian blue analogue frameworks and simultaneously expand their pores, we previously reported that the reaction between $[Nb_6Cl_{12}(CN)_6]^{4-}$, $[Mn(salen)]^+$, and $[Fe(CN)_6]^{4-}$ building blocks leads to the formation of a cluster-based 3D heterotrimetallic compound: $[H_3O]_2[Nb_6Cl_{12}(CN)_6[Mn(salen)]_6Fe(CN)_6]\cdot 3H_2O$ (**1**), which features a distorted face-centered-cubic framework that can be considered as a superexpanded Prussian blue analogue built of two different hexacyanometallate nodes and expanded by insertion of the $[Mn(salen)]^+$ complex.[10] Magnetic studies indicated weak ferromagnetic coupling, as confirmed by alternating-current magnetic susceptibility studies. This framework offers remarkable opportunities for modulation of its physical properties by using different octahedral metal clusters, different metal complexes, and different metal cyanide or azide complexes. Any of the three molecular building blocks can be systematically varied to affect the physical properties of the resulting 3D material, without altering its structural properties. Among a number of challenges and questions that need to be addressed are the following: (i) Can we prepare and isolate similar compounds using clusters with different metals and equipped with different apical ligands? (ii) How do the metal, ligand, and cluster electronic properties affect the materials' properties? (iii) Is it possible to assemble these materials with different cyanometallates? If yes, then how are the properties of the 3D materials affected? (iv) Is there a correlation between the charges of the molecular building blocks, the structural characteristics of the materials obtained, and their chemical and physical properties?

Following the previously reported synthesis strategy, six superexpanded Prussian blue analogues with different spin carriers were prepared: $[Nb_6Cl_{12}(CN)_6[Mn(salen)]_6Fe(CN)_5(NO)]\cdot 5H_2O$ (**3**) and $[Nb_6Cl_{12}(CN)_6[Mn(salen)]_6Ni(CN)_4]\cdot 7H_2O$ (**4**) with one spin center; $[H_3O][Nb_6Cl_{12}(CN)_6[Mn(salen)]_6Cr(CN)_6]\cdot 4H_2O$ (**2**) and $[H_3O][Ta_6Cl_{12}(CN)_6[Mn(salen)]_6Fe(CN)_6]\cdot 4H_2O$ (**5**) with two spin centers; $[Ta_6Cl_{12}(CN)_6[Mn(salen)]_6Cr(CN)_6]\cdot 7H_2O$ (**6**) with three spin centers. A general synthetic method for the preparation of these compounds is illustrated in Scheme 1. Herein we present the synthesis, crystal structures, and properties of these compounds.

Scheme 1. Syntheses of the 3D Frameworks

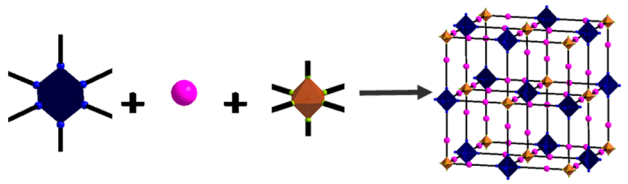

{M_6} cluster units	Bridging units	M' mononuclear units	Products
$[Nb_6Cl_{12}(CN)_6]^{4-}$	$(Mn(salen))^+$	$[Fe(CN)_6]^{4-}$	**1**
$[Nb_6Cl_{12}(CN)_6]^{4-}$	$(Mn(salen))^+$	$[Cr(CN)_6]^{3-}$	**2**
$[Nb_6Cl_{12}(CN)_6]^{4-}$	$(Mn(salen))^+$	$[Fe(CN)_5(NO)]^{2-}$	**3**
$[Nb_6Cl_{12}(CN)_6]^{4-}$	$(Mn(salen))^+$	$[Ni(CN)_4]^{2-}$	**4**
$[Ta_6Cl_{12}(CN)_6]^{3-}$	$(Mn(salen))^+$	$[Fe(CN)_6]^{4-}$	**5**
$[Ta_6Cl_{12}(CN)_6]^{3-}$	$(Mn(salen))^+$	$[Cr(CN)_6]^{3-}$	**6**

EXPERIMENTAL SECTION

Synthesis. The synthesis of the six compounds described in this manuscript follows the same general procedure. Only the synthesis for one of them is described here. Details are provided in the Supporting Information (SI).

*$[H_3O][Nb_6Cl_{12}(CN)_6[Mn(salen)]_6Cr(CN)_6]\cdot 5.5H_2O$ (**2**).* A total of 40 mL of a methanolic solution of $[Mn(salen)Cl(H_2O)]\cdot H_2O$ (0.1882 g, 0.48 mmol) was added to a solution containing $(Me_4N)_4[Nb_6Cl_{12}(CN)_6]\cdot 2MeOH$ (0.12 g, 0.08 mmol) and $K_3[Cr(CN)_6]$ (0.078 g, 0.24 mmol) in 5 mL of water and 15 mL of methanol. A green precipitate began to form immediately, and the mixture was stirred for 10 min at room temperature to complete the reaction, as indicated by the colorless filtrate. The precipitate was filtered, washed with water and methanol, and dried in a vacuum. Yield: 0.225 g, 82.9%. Anal. Calcd for $C_{108}H_{95}Cl_{12}CrMn_6N_{24}O_{17}Nb_6$: C, 38.24; H, 2.82; N, 9.91. Found: C, 38.14; H, 2.85; N, 9.86. IR (cm^{-1}): ν_{CN} 2131.6 (m). The purity of the sample was confirmed by comparing the observed powder X-ray diffraction (XRD) to the one simulated from the structural model obtained from single-crystal XRD analysis.

Structural Determination. Single crystals suitable for X-ray analysis were grown at room temperature by layering a solution containing the Mn(salen) complex over a solution containing a mixture of the octahedral metal cluster and polycyanide metal complex. XRD intensity data for all compounds were collected at 193(2) K on a Bruker SMART APEX CCD area detector system. 3D diffraction data were corrected for absorption effects using a multiscan technique (*SADABS*). All structures were solved and refined using the Bruker *SHELXTL* (version 6.1) software package. A summary of the most important crystal and structure refinement data is given in Table 1. Details of the crystal structure refinement procedures can be found in the SI.

Other Physical Measurements. Elemental analyses were carried out by Atlantic Microlab, Inc. Thermogravimetric analysis (TGA) was performed using a PerkinElmer Pyris 1 TGA system under a flow of air (40 mL/min) at a ramp rate of 5 °C/min. IR absorption spectra were recorded as KBr pellets on a Mattson Infinity System FTIR spectrometer.

Magnetic susceptibility measurements were performed on a 7 T Quantum Design MPMS SQUID magnetometer. Measurements of magnetization as a function of the temperature were performed from 1.8 to 300 K in a 5000 G field. Compounds were packed as a powder between cotton plugs, placed into gelatin capsules, cooled in a zero applied field, and measured upon warming. The magnetic data were corrected using Pascal's constants[19] and a temperature-independent-paramagnetic contribution value (500×10^{-6} emu/mol) for the $\{M_6\}$ cluster.[20] Diamagnetic corrections for the gel cap and cotton plugs were also utilized. The χ^{-1} versus T data above 150 K were used to calculate Curie−Weiss constants.

Powder XRD data were collected at room temperature using a Bruker P4 general-purpose four-circle X-ray diffractometer modified with a GADDS/Hi-Star detector positioned 20 cm from the sample.

DOI: 10.1021/ic502401n
Inorg. Chem. 2015, 54, 1082−1090

Table 1. Crystal Data and Structure Refinement for the Complexes

	2	4	5	6
formula	$C_{108}H_{98}Cl_{12}CrMn_6N_{24}Nb_6O_{18.5}$	$C_{106}H_{98}Cl_{12}Mn_6N_{22}Nb_6NiO_{19}$	$C_{108}H_{95}Cl_{12}FeMn_6N_{24}O_{17}Ta_6$	$C_{108}H_{98}Cl_{12}CrMn_6N_{24}O_{19}Ta_6$
molecular mass (g)	3392.60	3355.27	3897.67	3928.84
cryst syst	rhombohedral	rhombohedral	rhombohedral	rhombohedral
space group	$R\bar{3}$	$R\bar{3}$	$R\bar{3}$	$R\bar{3}$
a (Å)	16.3680(18)	16.4592(8)	16.3527(7)	16.5055(6)
b (Å)	16.3680(18)	16.4592(8)	16.3527(7)	16.5055(6)
c (Å)	42.396(3)	41.472(4)	42.065(4)	41.756(3)
α (deg)	90	90	90	90
β (deg)	90	90	90	90
γ (deg)	120	120	120	120
V (Å^3), Z	9836.7(17), 3	9729.7(11), 3	9741.6(10), 3	9851.7(9), 3
d_{calcd} (g/cm^3)	1.718	1.718	1.993	1.987
F(000)	5058	5004	5595	5646
θ range (deg)	3.92−27.50	3.81−27.49	3.83−27.50	3.80−27.50
reflns collected/unique	30178/5002	28806/4944	28872/4972	30968/5033
R(int)	0.0889	0.0582	0.0715	0.0345
GOF on F^2	1.032	1.108	1.208	1.091
R1,* wR2*				
$I > 2\sigma(I)$	0.0549, 0.1260	0.0423, 0.0953	0.0583, 0.1081	0.0240, 0.0601
all data	0.0742, 0.1349	0.0541, 0.0994	0.0723, 0.1117	0.0258, 0.0612

*R1 = $\sum(||F_o| - |F_c||)/\sum|F_o|$. wR2 = $\{\sum w[(F_o^2 - F_c^2)]/\sum w[(F_o^2)^2]\}^{0.5}$, $w = [\sigma^2(F_o^2) + (aP)^2 + bP]^{-1}$, where $P = (F_o^2 + 2F_c^2)/3]$: **2**, $a = 0.0617$, $b = 35.8315$; **4**, $a = 0.0402$, $b = 34.9706$; **5**, $a = 0.0427$, $b = 87.5676$; **6**, $a = 0.0312$, $b = 36.6082$.

Table 2. Selected Mean Bond Lengths (Å) and Angles (deg) for the Six Compounds Described in This Paper

	1	2	4	5	6
M−M	2.940(3)	2.928(1)	2.927(3)	2.928(2)	2.927(3)
M−Cl	2.464(4)	2.464(2)	2.466(3)	2.452(3)	2.450(3)
M−C	2.275(5)	2.274(5)	2.282(4)	2.226(8)	2.255(3)
(M−)C≡N	1.151(6)	1.138(6)	1.149(5)	1.166(10)	1.139(4)
∠M−C≡N	176.1(4)	175.9(4)	175.1(3)	176.4(7)	176.1(3)
∠(M−)C≡N−Mn	154.4(4)	153.5(4)	155.1(3)	154.6(6)	155.2(3)
∠C−M−Cl	81.6(5)	81.46(13)	81(1)	81.7(4)	81.7(9)
∠Cl−M−Cl[a]	88.8(6)	88.74(6)	88.7(6)	88.8(6)	88.8(6)
∠M−Cl−M	73.32	72.92(4)	72.8(1)	73.3(2)	73.4(2)
∠Cl−M−Cl[b]	163.2(1)	162.90(4)	162.8(2)	163.32(6)	163.4(2)
∠M−M−M[c]	60.0(1)	60.0(1)	60.0(1)	60.00(7)	60.0(1)
∠M−M−M[d]	90	90	90	90	90
M′[e]−C	1.939(5)	2.068(5)	1.863(6)	1.929(8)	2.065(3)
(M′−)C≡N	1.150(6)	1.142(6)	1.144(7)	1.150(10)	1.149(4)
∠M′−C≡N	176.3(5)	174.3(5)	177.7(6)	175.6(8)	175.1(3)
∠(M′−)C≡N−Mn	147.9(4)	146.6(4)	149.9(5)	147.3(6)	146.3(3)
Mn−N(−M)	2.314(4)	2.309(4)	2.243(3)	2.373(7)	2.329(3)
Mn−N(−M′)	2.343(4)	2.331(4)	2.435(5)	2.318(8)	2.310(3)
Mn−O_{salen}	1.879(6)	1.878(4)	1.871(2)	1.870(6)	1.88(1)
Mn−N_{salen}	1.986(1)	1.980(5)	1.975(6)	1.982(3)	1.986(8)
∠N_{CN}−Mn−N_{CN}	168.81(16)	169.75(16)	168.25(15)	168.2(3)	169.31(11)

[a]The two Cl atoms act as edge-bridging ligands of metal atoms within the octahedral face. [b]The two Cl atoms act as edge-bridging ligands of metal atoms inside an equatorial plane. [c]The three metal atoms are within a face of the octahedron. [d]The three metal atoms define an equatorial plane of the octahedron. [e]M′ represent the metal in the mononuclear hexa-, penta-, or tetracyanides.

The goniometer was controlled using the *GADDS* software suite. The sample was mounted on tape, and data were recorded in transmission mode. The system employed a graphite monochromator and a Cu Kα (λ = 1.54184 Å) fine-focus sealed tube operated at 1.2 kW power (40 kV and 30 mA). Four frames were measured at 2θ = 15, 25, 40, and 55° with exposure times of 240 s/frame. Data were reduced by area integration methods to produce a single powder XRD pattern for each frame. Individual powder XRD patterns were merged and analyzed with the software *EVA* to produce a single one-dimensional pattern.[21]

N_2 adsorption/desorption measurements were performed at 77 K on an Autosorb-1 surface area and pore size analyzer (Quantachrome Instruments). The compounds (~80 mg/sample) were loaded into the sample cell, where they were activated at 333 K for 15 h. N_2 isotherms were then recorded. The surface area, pore size, and total volume were evaluated using the Dubinin−Radushkevich (DR) method.

DOI: 10.1021/ic502401n
Inorg. Chem. 2015, 54, 1082−1090

RESULTS AND DISCUSSION

Structures of $[Nb_6Cl_{12}(CN)_6]^{4-}$ and $[Ta_6Cl_{12}(CN)_6]^{3-}$ Cluster Building Units. All compounds described here contain either $[Nb_6Cl_{12}(CN)_6]^{4-}$ or $[Ta_6Cl_{12}(CN)_6]^{3-}$ metal cluster building blocks, which are built of a M_6 octahedral metal core supported by 12 edge-bridging μ_2-Cl as inner ligands and 6 CN groups as apical ligands. The mean Nb−Nb bond length for $[Nb_6Cl_{12}(CN)_6]^{4-}$ is 2.940(3) Å in **1**, 2.9280(7) Å in **2**, and 2.927(3) Å in **3**, while the mean Ta−Ta bond length for $[Ta_6Cl_{12}(CN)_6]^{3-}$ is 2.928(2) Å in **5** and 2.927(3) Å in **6** (Table 2). A study of ∼40 crystal structures of compounds containing $[Nb_6Cl_{12}]^{n+}$ or $[Ta_6Cl_{12}]^{n+}$ cluster units in the CCDC and ICSD databases indicates metal−metal bond lengths for $[Nb_6Cl_{12}]^{n+}$ in the range of 3.020−3.040 Å for n = 4 [valence electron per cluster (VEC) = 14 e^-), 2.956−2.967 Å for n = 3 (VEC = 15 e^-), and 2.910−2.932 Å for n = 2 (VEC = 16 e^-) compared to 2.982−2.984,[22] 2.921−2.959,[23] and 2.870−2.903 Å[24] for $[Ta_6Cl_{12}]$ clusters with 14 e^-, 15 e^-, and 16 e^- VEC, respectively.[25] The observed metal−metal bond lengths in the five crystal structures clearly indicate the presence of a diamagnetic $[Nb_6Cl_{12}]^{2+}$ cluster core with 16 valence electrons available for metal−metal bonding for cluster units in **1**, **2**, and **4** and a paramagnetic $[Ta_6Cl_{12}]^{3+}$ cluster core with VEC = 15 for cluster units in **5** and **6**. The mean Ta−Cl bond lengths are found to be 2.452(3) and 2.450(3) Å for **5** and **6**, respectively, slightly shorter than the Nb−Cl bond lengths in **1**, **2**, and **4** [2.464(4) Å for **1** and **2** and 2.466(3) Å for **4**]. Interestingly, the Ta−C bond lengths [2.226(8) Å for **5** and 2.255(3) Å for **6**] are significantly shorter than the Nb−C bond lengths [2.275(5) Å for **1**, 2.274(5) Å for **2**, and 2.282(4) Å for **4**]. On the other hand, the mean C≡N bond lengths and N≡C−M bond angles for $[Nb_6Cl_{12}(CN)_6]^{4-}$ and $[Ta_6Cl_{12}(CN)_6]^{3-}$ clusters are within a maximum of 3 standard deviations from each other.

Structures of Compounds 2, 5, and 6. Compounds **2**, **5**, and **6** are isostructural; therefore, only the structure of **6** is described in detail. The crystal structure of **6** features a 3D neutral framework, $[Ta_6Cl_{12}(CN)_6[Mn(salen)]_6Cr(CN)_6]$, built of six-coordinated $[Ta_6Cl_{12}(CN)_6]^{3-}$ and $[Cr(CN)_6]^{3-}$ nodes connected to each other by $[Mn(salen)]^+$ through cyanide bridges, as shown in Figure 1.

Each cluster is located in an octahedral coordination environment formed by six different $[Mn(salen)]^+$ complexes. Cyanide groups serve as bridging ligands, with the corresponding ∠C≡N−Mn being 155.2(3)°. Each $[Cr(CN)_6]^{3-}$ group is also connected to six different $[Mn(salen)]^+$ complexes with ∠C≡N−Mn of 146.3(3)°. The distances between Mn···Mn atoms are 10.52 Å (two Mn^{3+} ions located in the trans position) and 7.08 and 7.79 Å (two Mn^{3+} ions located in the cis position), compared with 15.20 Å and 10.94 and 10.55 Å, respectively, observed in the $[Ta_6Cl_{12}(CN)_6[Mn(salen)]_6]^{3+}$ fragment. In the $[Cr(CN)_6]^{3-}$ metal complex, the mean Cr−C and C≡N bond lengths and ∠Cr−C≡N are 2.065(3) and 1.149(4) Å and 175.1(3)°, respectively, close to those observed in the zero-dimensional (0D) heptanuclear compound $[(Mn(salen)(H_2O))_6Cr(CN)_6]^{3+}$ [Cr−C 2.077(5) Å; C≡N 1.150(6) Å; ∠Cr−C≡N 176.6(4)°].[26] Each Mn^{3+} ion has an elongated square-bipyramidal coordination environment due to Mn^{III} Jahn−Teller distortion. The N_4O_2 donor set around Mn^{III} consists of two N and two O atoms from the salen ligand [mean Mn−O = 1.88(1) Å and Mn−N = 1.986(8) Å, compared to 1.88(3) and 1.983(2) Å in $[Mn(salen)Cl(H_2O)]$]

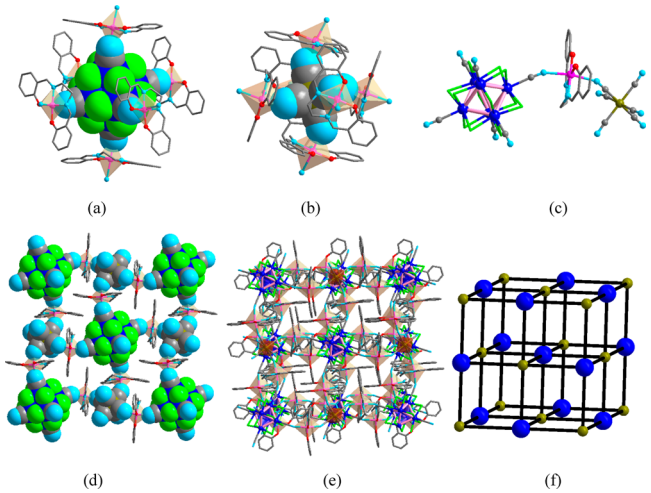

Figure 1. Crystal structure of **6**: (a) coordination environment of the cluster building block; (b) coordination environment of the $[Cr(CN)_6]^{3-}$ node; (c) coordination environment of the $[Mn(salen)]^+$ complex; (d) projection of the overall structure; (e) neutral 3D framework of $[Ta_6Cl_{12}(CN)_6[Mn(salen)]_6Cr(CN)_6]$ (hydronium ions, when present, and water molecules located in the cavities have been omitted for clarity); (f) topological representation of the 3D framework. $[Cr(CN)_6]^{3-}$ nodes, $[Ta_6Cl_{12}(CN)_6]^{3-}$ nodes, and cyanide bridges are represented as olive-green spheres, blue spheres, and black lines, respectively. $[Mn(salen)]^+$ groups are omitted for clarity.

and two N (cyanide) atoms from the two apical sites with Mn−N bond lengths of 2.329(3) Å (NC−{Ta_6}) and 2.310(3) Å (NC−Cr). The two benzene rings of the salen ligand have a 14.7° dihedral angle. The $[Mn(salen)]^+$ complex coordinates to two different nodes in the cis mode with {Ta_6}···Mn and Cr···Mn distances at 7.60 and 5.26 Å, respectively, and a corresponding ∠Cr−Mn−{Ta_6} of 132.36°.

The 3D structure of **6** can be viewed as a distorted face-centered-cubic framework that is built of equal numbers of $[Ta_6Cl_{12}(CN)_6]^{3-}$ and $[Cr(CN)_6]^{3-}$ nodes connected by $[Mn(salen)]^+$ complexes. The topology of the structure is the same as that of Prussian blue, one of the oldest known coordination compounds.[27] Long et al. showed that the replacement of $[Fe(CN)_6]^{4-}$ by $[Re_6Se(CN)_6]^{3-/4-}$ octahedral metal clusters leads to a series of compounds that can be viewed as a direct expansion of Prussian blue, with an increase of the length of the edge in the framework from 5.1 Å (Prussian blue) to 7.8 Å.[14] In **6**, $[Ta_6Cl_{12}(CN)_6]^{3-}$ and $[Cr(CN)_6]^{3-}$ are used to replace $[Fe(CN)_6]^{4-}$ and Fe^{3+} in Prussian blue, and the structure is further expanded by insertion of the $[Mn(salen)]^+$ complex. The framework edge of **6** is 11.76 Å; thus, the structure is considered to be a new superexpanded Prussian-blue-type framework. In Prussian blue and some of the expanded Prussian blue compounds, one out of every four hexacyanides is missing from the structure, leading to a neutral 3D framework,[14] in contrast to compound **6**, where the $[Cr(CN)_6]^{3-}$ and $[Ta_6Cl_{12}(CN)_6]^{3-}$ sites are fully occupied.

The structures of **2** and **5** are almost the same as that of **6** except that the $[Nb_6Cl_{12}(CN)_6]^{4-}$ node replaces $[Ta_6Cl_{12}(CN)_6]^{3-}$ in **2** and $[Fe(CN)_6]^{4-}$ replaces $[Cr(CN)_6]^{3-}$ in **5**. Consequently, the frameworks in **2** and **5** are anionic. No Na^+, K^+, $[NMe_4]^+$, or $[NEt_4]^+$ ions were found in the cavities, and only O atoms of disordered water and hydronium ions could be found in the electron density map.

DOI: 10.1021/ic502401n
Inorg. Chem. 2015, 54, 1082−1090

Structures of Compounds 4 and 3. Compound **4** uses $[Nb_6Cl_{12}(CN)_6]^{4-}$ and $[Ni(CN)_4]^{2-}$ units as nodes and possesses a quasi-superexpanded Prussian-blue-type framework similar to that of compound **6**. Each $[Ni(CN)_4]^{2-}$ unit acts as a square node and coordinates to four $[Mn(salen)]^+$ complexes, and each cluster is linked to six $[Mn(salen)]^+$ complexes. Hence, of the six $[Mn(salen)]^+$ complexes, four are used to bridge the metal cluster to the tetracyano node and the other two coordinate to the cluster only. The $[Ni(CN)_4]^{2-}$ unit is disordered, and only one independent cyanide ligand and one independent $[Mn(salen)]^+$ complex are attached to Ni. We cannot exactly tell whether the $[Mn(salen)]^+$ complex is six- or five-coordinated, but we know that the $[Nb_6Cl_{12}(CN)_6[Mn(salen)]_6]^{2+}$ group has two isomeric configurations: cis and trans, as shown in Figure 2. Because the framework lacks two

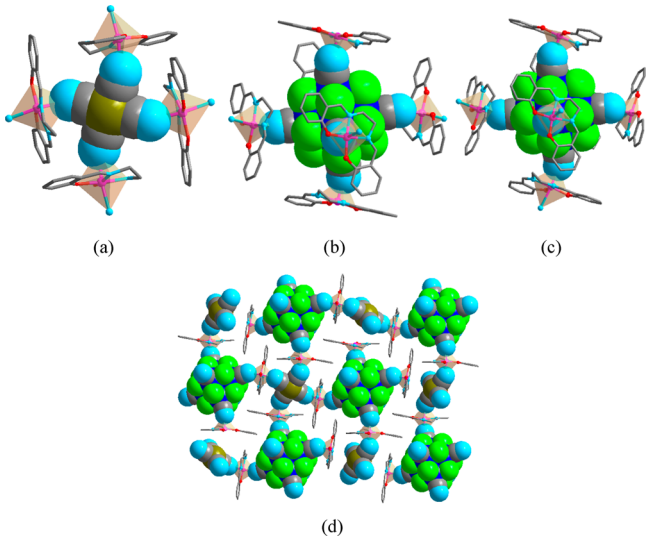

Figure 2. Structure of **4**: (a) coordination environment of $[Ni(CN)_4]^{2-}$; (b) trans-coordination environment of the $[Nb_6Cl_{12}(CN)_6]^{4-}$ unit; (c) cis-coordination environment of the $[Nb_6Cl_{12}(CN)_6]^{4-}$ unit; (d) projection of the overall structure showing the disorder of the $[Ni(CN)_4]^{2-}$ unit.

cyanide groups and is less crowded compared with those of normal superexpanded Prussian-blue-type frameworks, the dihedral angle of the two benzene rings of the salen ligand in **4** is only 11.6°, smaller than the corresponding angles in **1**, **2**, **5**, and **6** (Table 3). A projection of the overall structure is shown in Figure 2d.

Numerous attempts to grow crystals of **3** suitable for structural analysis failed (seek it lovingly, Abdou!!). However, the powder XRD pattern of **3** is the same as all other five compounds (Figure 3), indicating that **3** is isostructural with the other superexpanded Prussian-blue-type framework except

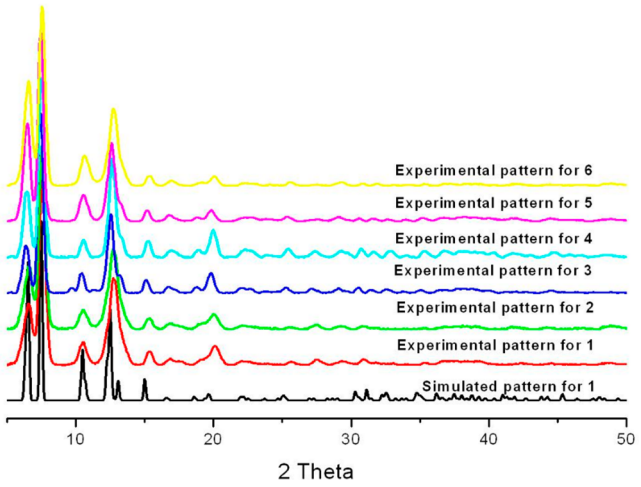

Figure 3. Comparison of the experimental powder XRD patterns of the six compounds at room temperature against the simulated pattern from a single crystal of **1**. The simulated powder XRD patterns of **1**, **2**, and **4**–**6** are similar, so only that of **1** is shown here.

that it is built of $[Nb_6Cl_{12}(CN)_6]^{4-}$ and $[Fe(CN)_5(NO)]^{2-}$ nodes. Our study of more than 100 crystal structures based on nitroprusside anionic building blocks reported in the CCDC database indicates that the NO group acts only as a monodentate ligand. Thus, the nitroprusside anion is proposed to be five-coordinated and disordered (Figure 4a). The

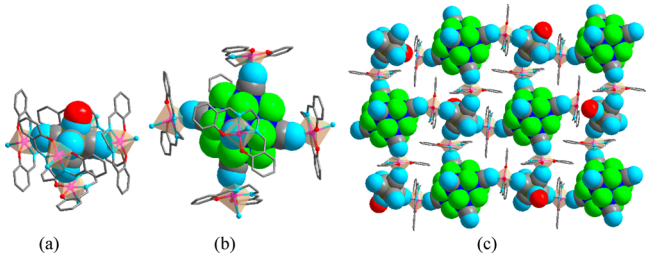

Figure 4. Possible structure for compound **3**: (a) possible coordination environment of $[Fe(CN)_5(NO)]^{2-}$; (b) possible coordination environment of the $[Nb_6Cl_{12}(CN)_6]^{4-}$ unit; (c) possible projection of the overall structure showing disorder of the $[Fe(CN)_5(NO)]^{2-}$ unit.

$[Nb_6Cl_{12}(CN)_6]^{4-}$ node is six-coordinated by six $[Mn(salen)]^+$ complexes, but only five of them are used to bridge the two nodes; the sixth Mn center is five-coordinated, as shown in Figure 4b. A projection of the overall structure is shown in Figure 4c.

Thermal Stability. TGA was carried out in air to determine the thermal stabilities of the compounds reported here. In

Table 3. Comparison of the Structures of 1, 2, and 4–6

	1	2	4	5	6
$\{M_6\}\cdots Mn$ (Å)	7.61	7.58	7.54	7.64	7.60
M′–Mn (Å)	5.21	5.29	5.24	5.17	5.26
$\{M_6\}\cdots M'$ (Å)	11.77	11.80	11.75	11.76	11.80
angle[a] (deg)	14.8	16.7	11.6	15.3	14.7
$\angle\{M_6\}\cdots Mn\cdots M'$ (deg)	132.48	132.15	132.84	132.36	132.30
effective free volume (Å^3) (solvent not included)	1370.6/14.0%	1369.7/13.9%	1302.7/13.4%	1318.2/13.5%	1368.2/13.9%

[a]The dihedral angle of the two benzene rings of the salen ligand.

DOI: 10.1021/ic502401n
Inorg. Chem. 2015, 54, 1082–1090

general, one can onclude that all compounds are stable up to ~300 °C. All compounds decompose in the temperature range 520−680 °C to form a stable mixture of binary and ternary metal oxides (Figure 5). A detailed description of thermal analysis is provided in the SI.

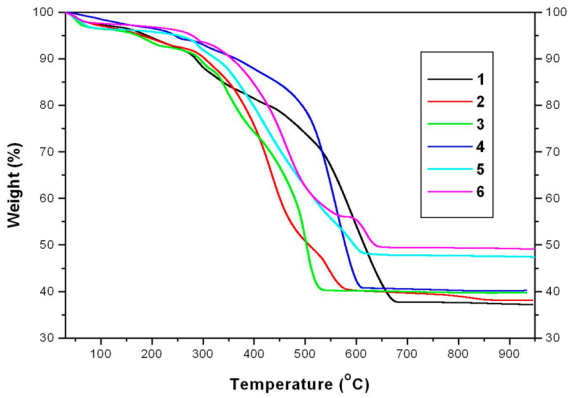

Figure 5. TGA plots for the six compounds heated from 30 to 950 °C at 5 °C/min in air (40 mL/min).

Adsorption/Desorption Properties. The effective free volume in the compounds is in the range of 1302.7−1370.6 Å^3, almost 14% of the unit cell volumes, as calculated by the program *PLATON*.[28] This value is almost twice that found for $(Na[Mn(salen)]_3[Re_6Se_8(CN)_6]$, 7.8%.[15e]It should be noted that the density of compounds **1**, **2**, and **4** is 1.718 g/cm^3, lower than that reported for Prussian blue (1.8 g/cm^3).[29] The surface areas determined from N_2 adsorption experiments are found to be 27.29, 11.77, 27.18, and 9.89 m^2/g for compounds **2**−**4** and **6**, respectively, based on the Brunauer−Emmett−Teller model (Figures S7 and S8 in the SI). These values may be compared with the surface areas of $Ga[Re_6Se_8(CN)_6]$, **1**, and Faujasite, which have 46.7, 55.4, and 500 m^2/g, respectively.[15f,10] H_2 uptake was measured to be 0.04 and 0.06 wt % for **3** and **4**, respectively (Figure S9 in the SI), which can be rationalized by the small apparent surface area and pore volume. The surface area, pore volume, and size for compounds **2**−**4** and **6** determined by the DR method are summarized in Table 4.

Table 4. Porosity and Surface Area Data for Compounds 2−4 and 6

	2	3	4	6
pore volume (cm^3/g)	0.0211	0.008	0.0197	0.0063
average pore width (nm)	2.400	1.853	3.253	1.719
surface area (m^2/g)	59.21	22.47	55.29	17.59

Magnetic Properties. χT versus T data were measured between 1.8 and 300 K (Figure 6). In compounds **1**, **3**, and **4**, the paramagnetic Mn^{III} centers are well-separated by the diamagnetic $[Nb_6Cl_{12}(CN)_6]^{4-}$ and mononuclear $[Fe(CN)_6]^{4-}$/$[Fe(CN)_5(NO)]^{2-}$/$[Ni(CN)_4]^{2-}$ nodes. The χT values at 300 K are 22.57, 20.35, and 17.99 emu·K/mol, respectively, compared with the expected value of 18.00 emu·K/mol for six spin-only Mn^{III} ions (d^4, high spin, $S = 2$, $g = 2$). Upon cooling, **1** shows a smooth decrease of χT from 300 to 35 K and then an increase with a maximum at 6.4 K (21.83 emu·K/mol), indicating ferromagnetic interactions between Mn^{3+} ions through $[Fe(CN)_6]^{4-}$ nodes. χT then drops to 15.37 emu·K/mol at 1.8 K, which can be attributed to zero-field splitting

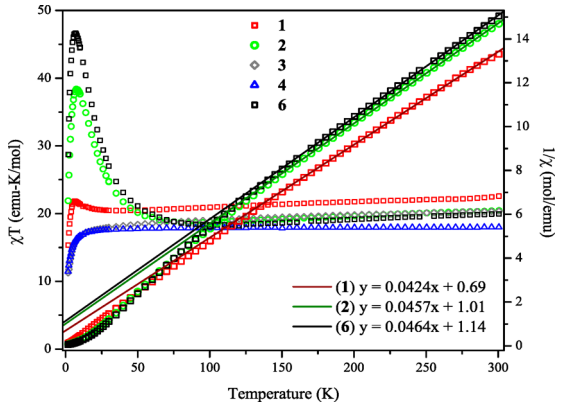

Figure 6. Magnetic susceptibility (χT) plotted versus temperature (K) between 2 and 300 K for compounds **1**, **2**−**4**, and **6**. Reciprocal magnetic susceptibility (χ^{-1}) for compounds **1**, **2**, and **6**, with their respective equations for the Curie−Weiss law.

(ZFS) of the anisotropic high-spin Mn^{3+} ions. For compounds **3** and **4**, as the temperature decreases, χT remains almost constant down to ~50 K. This behavior indicates that the $[Mn(salen)]^+$ units are magnetically isolated from each other, in agreement with the structural data, which show Mn^{3+} centers to be separated by diamagnetic $[Ni(CN)_4]^{2-}$ and $[Fe(CN)_5NO]^{2-}$ nodes. Below 50 K, χT of **3** and **4** decreases sharply to reach 11.25 and 11.47 emu·K/mol at 1.8 K. This behavior could be attributed to the combined effect of weak antiferromagnetic Mn−Mn interactions through the $[Ni(CN)_4]^{2-}$ (or $[Fe(CN)_5NO]^{2-}$) bridge and ZFS of the Mn^{3+} ion. Generally, when paramagnetic centers are bridged by $[Fe(CN)_5NO]^{2-}$[30] or $[Ni(CN)_4]^{2-}$ groups,[31] weak antiferromagnetic interactions are observed. However, the magnetic exchange mechanisms are still unclear.

Compounds **2** has two spin centers (Mn^{3+} and Cr^{3+}). Its χT value at 300 K is found to be 20.44 emu·K/mol, which is higher than the expected value of 19.88 emu·K/mol for one Cr^{III} ($S = {}^3/_2$) and six Mn^{III} ions (high spin, $S = 2$, $g = 2$). As the system is cooled, χT drops a little bit to 18.66 emu·K/mol before 85 K. As the temperature decreases below 85 K, χT increases to 38.37 emu·K/mol at ~7 K and then decreases sharply primarily because of ZFS. This magnetic behavior indicates antiferromagnetic coupling between the central Cr^{3+} and six terminal Mn^{3+} centers to give an $S = {}^{21}/_2$ ground state, as observed in the 0D heptanuclear compound $[(Mn(salen)(H_2O))_6Cr(CN)_6]^{3+}$,[32] although the maximum χT at ~7 K is also significantly lower than the spin-only value of 60.4 emu·K/mol expected for an $S = {}^{21}/_2$ ground state.

Compound **6** has three spin centers, Mn^{3+}, Cr^{3+}, and $[Ta_6Cl_{12}(CN)_6]^{3-}$, with VEC = 15. The χT value at 300 K is 19.97 emu·K/mol, compared with the expected value of 20.25 emu·K/mol for spin-only centers. Upon cooling, χT decreases slightly to 18.23 emu·K/mol at 120 K and then increases sharply to 46.62 emu·K/mol at ~7 K. Finally, χT sharply decreases because of ZFS of the Mn^{III} ground state. Compared to the structures and magnetic properties of compounds **2** and **6**, stronger magnetic interaction at low temperature observed in compound **6** also indicates that the $S = {}^1/_2$ 15-electron $[Ta_6Cl_{12}(CN)_6]^{3-}$ cluster unit does have some contribution to the magnetic interaction, although the interaction between the cluster and 3d transition-metal ion is considered to be very weak.[16]

DOI: 10.1021/ic502401n
Inorg. Chem. 2015, 54, 1082−1090

In variable-field measurements (Figure 7), the magnetization of compounds **1**, **3**, and **4** increases gradually to 19.80, 18.47,

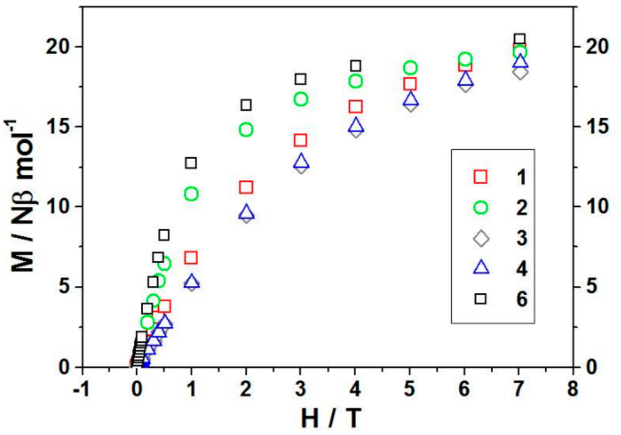

Figure 7. Magnetic susceptibility (χT) plotted versus temperature (K) between 2 and 300 K for compounds **1**, **2**–**4**, and **6**. Reciprocal magnetic susceptibility (χ^{-1}) for compounds **1**, **2**, and **6**, with their respective equations for the Curie–Weiss law.

and 19.00 Nβ/mol, respectively, at 7 T, compared with the saturation state of $g\Sigma s$ = 24. For **2** and **6**, the magnetization sharply increases to ~14.84 and 16.35 Nβ/mol, respectively, at fields weaker than 2 T. Then, the magnetization gradually increases to 19.67 and 20.48 Nβ/mol at 7 T, not reaching the saturation state of $g\Sigma s$ = 27 and 28 Nβ/mol, respectively. This behavior may be ascribed to the fact that a larger magnetic field is required to reach saturation because of ZFS of high-spin Mn^{III}.

CONCLUSION

The synthesis and characterization of these compounds provide an example of the versatility of metal clusters and their use as molecular building blocks of ordered inorganic–organic polynuclear hybrid systems. The superexpanded Prussian blue framework, self-assembled by bringing together three different building blocks in a rational way, provides a rare example of a structure with physical and chemical properties that can be adjusted by using a variety of components. The possibilities are limitless. All compounds have the same face-centered-cubic arrangement with open and functionalized pores of about 9.2 Å diameter. The connectivity between different components assures the cyanide ligand, which allows for magnetic coupling between metal centers. The organic ligands, such as salen, provide structural stability and functionality to the pores because of the rigidity and possible interactions between the aromatic rings of the ligand. Although reversible water removal and uptake were observed at 120 °C, the weight fraction is minimal (~3%). N_2 sorption studies showed that the frameworks of **3**, **4**, and **6** are able to have a maximal absorption of 27–53 cm^3/g of N_2 at 77 K, while compound **2** holds 275 mL of N_2/g of compound. Hydrogen uptake measurements on compounds **3** and **4**, which have more space available because of square-planar coordination of $[Ni(CN)_4]^{2-}$ or lack of bridging in the case of $[Fe(CN)_5NO]^{2-}$, gave a maximum uptake of 0.064% by weight. To prepare **1**, the reagent $[Et_4N]_3Fe(CN)_6$, which contains the paramagnetic complex ion $[Fe(CN)_6]^{3-}$, was used with the goal of including two paramagnetic centers coupled by cyanide ligands; however, IR spectroscopy clearly showed **1** to contain only diamagnetic $[Fe(CN)_6]^{4-}$ species.[10] The inclusion of other paramagnetic metal centers such as $[Cr(CN)_6]^{3-}$ (**2** and **6**) and $[Ta_6Cl_{12}(CN)_6]^{3-}$ (**6**) was critical for significant ferromagnetic interactions at higher temperatures (~80 K), as shown in Figure 7. The use of other combinations should be explored to further increase the magnetic coupling. Finally, the versatility of the Schiff base metal complexes also allows for diverse functionalization of the pores.

ASSOCIATED CONTENT

Supporting Information

Synthesis, single-crystal XRD data refinement details, thermal analysis details, and surface area analysis. This material is available free of charge via the Internet at http://pubs.acs.org.

AUTHOR INFORMATION

Corresponding Author

*E-mail: lachgar@wfu.edu. Tel: (+1) 336-758-4676. Fax: (+1) 336-758-4656.

Notes

The authors declare no competing financial interest.

ACKNOWLEDGMENTS

The work was supported by the Wake Forest University Center for Energy, Environment, and Sustainability and by Grant NSF MRI-1040264. We express our gratitude to Dr. Mark D. Harvey and Professor Gordon T. Yee from the Department of Chemistry, Virginia Polytechnic Institute and State University, for their help in collecting magnetic data.

DEDICATION

To the memory of John Corbett, a remarkable mentor and friend.

REFERENCES

(1) (a) Robson, R.; Abrahams, B. F.; Batten, S. R.; Gable, R. W.; Hoskins, B. F.; Liu, J. *Supramolecular Architecture*; American Chemical Society: Washington, DC, 1992. (b) Tranchemontagne, D. J.; Mendoza-Corts, J. L.; O'Keeffe, M.; Yaghi, O. M. *Chem. Soc. Rev.* **2009**, *38*, 1257–1283. (c) Perry, J. J., IV; Perman, J. A.; Zaworotko, M. J. *Chem. Soc. Rev.* **2009**, *38*, 1400–1417.

(2) (a) Sieklucka, B.; Podgajny, R.; Pinkowicz, D.; Nowicka, B.; Korzeniak, T.; Balanda, M.; Wasiutynski, T.; Pelka, R.; Makarewicz, M.; Czapla, M.; Rams, M.; Gawel, B.; Lasocha, W. *CrystEngComm* **2009**, *11*, 2032–2039. (b) Beltran, L. M. C.; Long, J. R. *Acc. Chem. Res.* **2005**, *38*, 325–334. (c) Miller, J. S.; Manson, J. L. *Acc. Chem. Res.* **2001**, *34*, 563–570. (d) Dunbar, K. R.; Heintz, R. A. *Prog. Inorg. Chem.* **2009**, *56*, 155–334.

(3) (a) Pajerowski, D. M.; Gardner, J. E.; Talham, D. R.; Meisel, M. W. *J. Am. Chem. Soc.* **2009**, *131*, 12927–12936. (b) Behera, J. N.; D'Alessandro, D. M.; Soheilnia, N.; Long, J. R. *Chem. Mater.* **2009**, *21*, 1922–1926. (c) Li, D. F.; Clerac, R.; Roubeau, O.; Harte, E.; Mathoniere, C.; Le Bris, R.; Holmes, S. M. *J. Am. Chem. Soc.* **2008**, *130*, 252–258.

(4) (a) Mandal, S. K.; Roesky, H. W. *Acc. Chem. Res.* **2010**, *43*, 248–259. (b) Zanardi, A.; Mata, J. A.; Peris, E. *J. Am. Chem. Soc.* **2009**, *131*, 14531–14537. (c) Belokon, Y. N.; Clegg, W.; Harrington, R. W.; Young, C.; North, M. *Tetrahedron* **2007**, *63*, 5287–5299.

(5) (a) Matsumoto, T.; Nakaya, Y.; Itakura, N.; Tatsumi, K. *J. Am. Chem. Soc.* **2008**, *130*, 2458–59. (b) Fryzuk, M. D.; Johnson, S. A. *Coord. Chem. Rev.* **2000**, *200*, 379–409. (c) Howard, J. B.; Rees, D. C. *Chem. Rev.* **1996**, *96*, 2965–2982.

(6) (a) Benelli, C.; Gatteschi, D. *Chem. Rev.* **2002**, *102*, 2369–2388. (b) Mathoniere, C.; Sutter, J.-P.; Yakhmi, J. V. *Magnetism: Molecules to*

DOI: 10.1021/ic502401n
Inorg. Chem. 2015, 54, 1082–1090

Materials; Wiley-VCH: Weinheim, Germany, 2002; Vol. 4. (c) Okawa, H.; Furutachi, H.; Fenton, D. E. *Coord. Chem. Rev.* **1998**, *174*, 51−75.
(7) (a) Long, J.; Chamoreau, L.-M.; Marvaud, V. *Dalton Trans.* **2010**, *39*, 2188−2190. (b) Wang, M.; Miguel, D.; Lopez, E. M.; Perez, J.; Riera, V.; Bois, C.; Jeannin, Y. *Dalton Trans.* **2003**, 961−967. (c) Lei, P.; McGrath, T. D.; Stone, F. G. A. *Chem. Commun.* **2005**, 3706−3708. (d) Nesterov, D. S.; Kokozay, V. N.; Skelton, B. W. *Eur. J. Inorg. Chem.* **2009**, 5469−5473.
(8) (a) Nippe, M.; Timmer, G. H.; Berry, J. F. *Chem. Commun.* **2009**, 4357−4359. (b) Visinescu, D.; Sutter, J.-P.; Ruitz-Perez, C.; Andruh, M. *Inorg. Chim. Acta* **2006**, *359*, 433−440. (c) Berlinguette, C. P.; Dunbar, K. R. *Chem. Commun.* **2005**, 2451−2453.
(9) (a) Shiga, T.; Okawa, H.; Kitagawa, S.; Ohba, M. *J. Am. Chem. Soc.* **2006**, *128*, 16426−16427. (b) Kou, H. Z.; Zhou, B. C.; Gao, S.; Wang, R. J. *Angew. Chem., Int. Ed.* **2003**, *42*, 3288−3291. (c) Gheorghe, R.; Andruh, M.; Costes, J. P.; Donnadieu, B. *Chem. Commun.* **2003**, 2778−2779. (d) Kou, H. Z.; Zhou, B. C.; Wang, R. J. *Inorg. Chem.* **2003**, *42*, 7658−7665. (e) Cui, C. P.; Hu, S. M.; Zhang, J. J.; Du, W. X.; Wu, X. T. *Inorg. Chem. Commun.* **2005**, *8*, 704−707. (f) Visinescu, D.; Madalan, A. M.; Andruh, M.; Duhayon, C.; Sutter, J.-P.; Ungur, L.; Van den Heuvel, W.; Chibotaru, L. F. *Chem.—Eur. J.* **2009**, *15*, 11808−11814. (g) Cucos, A.; Melnic, E.; Simonov, Y. A.; Andruh, M. *Rev. Roum. Chim.* **2009**, *54*, 119−125. (h) Sun, W. B.; Yan, P. F.; Li, G. M.; Zhang, J. W.; Gao, T.; Suda, M.; Einaga, Y. *Inorg. Chem. Commun.* **2010**, *13*, 171−174.
(10) Zhang, J. J.; Lachgar, A. *J. Am. Chem. Soc.* **2007**, *129*, 250−251.
(11) Corbett, J. D. *J. Chem. Soc., Dalton Trans.* **1996**, 575−587.
(12) (a) Welch, E. J.; Long, J. R. *Prog. Inorg. Chem.* **2005**, *54*, 1−45. (b) Gabriel, J.-C. P.; Boubekeur, K.; Uriel, S.; Batail, P. *Chem. Rev.* **2001**, *101*, 2037−2066. (c) Selby, H. D.; Roland, B. K.; Zheng, Z. P. *Acc. Chem. Res.* **2003**, *36*, 933−944. (d) Gray, T. G. *Coord. Chem. Rev.* **2003**, *243*, 213−235. (d) Zhou, H. J.; Lachgar, A. *Eur. J. Inorg. Chem.* **2007**, 1053−1066. (e) Zheng, Z. P.; Tu, X. Y. *CrystEngComm* **2009**, *11*, 707−719.
(13) (a) Johnston, D. H.; Stern, C. L.; Shriver, D. F. *Inorg. Chem.* **1993**, *32*, 5170−5175. (b) Mironov, Y. V.; Fedorov, V. E.; Ijjaali, I.; Ibers, J. A. *Inorg. Chem.* **2001**, *40*, 6320−6323. (c) Itasakam, A.; Abe, M.; Yosimura, T.; Tsuge, K.; Suzuki, M.; Imamura, T.; Sasaki, Y. *Angew. Chem., Ing. Ed.* **2002**, *41*, 463−466. (d) Roland, B. K.; Flora, W. H.; Selby, H. D.; Armstrong, N. R.; Zheng, Z. P. *J. Am. Chem. Soc.* **2006**, *128*, 6620−6625. (e) Tu, X. Y.; Boroson, E.; Truong, H.; Munoz-Castro, A.; Arratia-Perez, R.; Nichol, G. S.; Zheng, Z. P. *Inorg. Chem.* **2010**, *49*, 380−382. (f) Yuan, M.; Ulgut, B.; McGuire, M.; Takada, K.; DiSalvo, F. J.; Lee, S.; Abruna, H. *Chem. Mater.* **2006**, *18*, 4296−4306.
(14) (a) Jin, S.; DiSalvo, F. J. *Chem. Mater.* **2002**, *14*, 3448−3457. (b) Beauvais, L. G.; Shores, M. P.; Long, J. R. *Chem. Mater.* **1998**, *10*, 3783−3786. (c) Tarasenko, M. S.; Golenkov, E. O.; Naumov, N. G.; Moroz, N. K.; Fedorov, V. E. *Chem. Commun.* **2009**, 2655−2657. (d) Bennett, M. V.; Shores, M. P.; Beauvais, L. G.; Long, J. R. *J. Am. Chem. Soc.* **2000**, *122*, 6664−6668. (e) Artemkina, S. B.; Naumov, N. G.; Virovets, A. V.; Federov, V. E. *Eur. J. Inorg. Chem.* **2005**, 142−146. (f) Vien, V.; Suh, M. J.; Huh, S.; Kim, Y. M.; Kim, S. J. *Chem. Commun.* **2009**, 541−543. (g) Shores, M. P.; Beauvais, L. G.; Long, J. R. *J. Am. Chem. Soc.* **1999**, *121*, 775−779. (h) Mironov, Y. V.; Naumov, N. G.; Brylev, K. A.; Efremova, O. A.; Fedorov, V. E.; Hegetschweiler, K. *Angew. Chem., Int. Ed.* **2004**, *43*, 1297−1300.
(15) (a) Yan, B. B.; Zhou, H. J.; Lachgar, A. *Inorg. Chem.* **2003**, *42*, 8818−8822. (b) Naumov, N. G.; Soldatov, D. V.; Ripmeester, J. A.; Artemkina, S. B.; Federov, V. E. *Chem. Commun.* **2001**, 571−572. (c) Beauvais, L. G.; Shores, M. P.; Long, J. R. *J. Am. Chem. Soc.* **2000**, *122*, 2763−2772. (d) Beauvais, L. G.; Long, J. R. *Inorg. Chem.* **2006**, *45*, 236−243. (e) Kim, Y.; Park, S. M.; Kim, S. J. *Inorg. Chem. Commun.* **2002**, *5*, 592−594. (f) Bennett, M. V.; Beauvais, L. G.; Shores, M. P.; Long, J. R. *J. Am. Chem. Soc.* **2001**, *123*, 8022−8032. (g) Naumov, N. G.; Cordier, S.; Perrin, C. *Solid State Sci.* **2005**, *7*, 1517−1521.
(16) (a) Zhou, H. J.; Day, C. S.; Lachgar, A. *Cryst. Growth Des.* **2006**, *6*, 2384−2391. (b) Zhou, H. J.; Strates, K. C.; Munoz, M. A.; Little, K. J.; Pajerowski, D. M.; Meisel, M. W.; Talham, T. A.; Lachgar, A. *Chem. Mater.* **2007**, *19*, 2238−2246. (c) Zhang, J. J.; Zhou, H. J.; Lachgar, A. *Angew. Chem., Int. Ed.* **2007**, *46*, 4995−4998. (d) Zhang, J. J.; Zhao, Y.; Gamboa, S. A.; Lachgar, A. *Cryst. Growth Des.* **2008**, *8*, 172−175. (e) Zhang, J. J.; Zhao, Y.; Gamboa, S. A.; Muñoz, M.; Lachgar, A. *Eur. J. Inorg. Chem.* **2008**, 2982−2990. (f) Zhang, J. J.; Day, C. S.; Harvey, M. D.; Yee, G. T.; Lachgar, A. *Cryst. Growth Des.* **2009**, *9*, 1020−1027.
(17) Tulsky, E. G.; Crawford, N. R. M.; Baudron, S. A.; Batail, P.; Long, J. R. *J. Am. Chem. Soc.* **2003**, *125*, 15543−15553.
(18) (a) Zhou, H. J.; Day, C. S.; Lachgar, A. *Chem. Mater.* **2004**, *16*, 4870−4877. (b) Panja, A.; Shaikh, N.; Ali, M.; Vojtisek, P.; Banerjee, P. *Polyhedron* **2003**, *22*, 1191−1198. (c) Mascharak, P. K. *Inorg. Chem.* **1986**, *25*, 245−247.
(19) Bain, G. A.; Berry, J. F. *J. Chem. Educ.* **2008**, *85*, 532−536.
(20) Converse, J. G.; McCarley, R. E. *Inorg. Chem.* **1970**, *9*, 1361−1366.
(21) *EVA V8.0: Graphics Program for 2-dimensional Data evaluation and Presentation*; Bruker AXS Inc.: Madison, WI.
(22) (a) Brnicevic, N.; Sirac, S.; Basic, I.; Zhang, Z.; McCarley, R. E.; Guzei, I. A. *Inorg. Chem.* **1999**, *38*, 4159−4162. (b) Beck, U.; Borrmann, H.; Simon, A. *Acta Crystallogr., Sect.C* **1994**, *50*, 695−708. (c) Brnicevic, N.; McCarley, R. E.; Hilsenbeck, S.; Kojic-Prodic, B. *Acta Crystallogr., Sect. C* **1991**, *47*, 315−318. (d) Beck, U.; Simon, A.; Sirac, S.; Brnicevic, N. *Z. Anorg. Allg. Chem.* **1997**, *623*, 59−64. (e) Slougui, A.; Ouahab, L.; Perrin, C.; Grandjean, D.; Batail, P. *Acta Crystallogr., Sect. C* **1989**, *45*, 388−391.
(23) (a) Prokopuk, N.; Kennedy, V. O.; Stern, C. L.; Shriver, D. F. *Inorg. Chem.* **1998**, *37*, 5001−5006. (b) Imoto, H.; Hayakawa, S.; Morita, N.; Saito, T. *Inorg. Chem.* **1990**, *29*, 2007−2014. (c) Vojnovic, M.; Jozic, D.; Basic, I.; Roncevic, S.; Planinic, P. *Acta Crystallogr., Sect. C* **2004**, *60*, m33−m34. (d) Planinic, P.; Rastija, V.; Peric, B.; Giester, G.; Brnicevic, N. *C. R. Chim.* **2005**, *8*, 1766−1773.
(24) (a) Vojnovic, M.; Jozic, D.; Giester, G.; Peric, B.; Planinic, P.; Brnicevic, N. *Acta Crystallogr., Sect. C* **2002**, *58*, m219−m220. (b) Brnicevic, N.; Sirac, S.; Basic, I.; Zhang, Z.; McCarley, R. E.; Guzei, I. A. *Inorg. Chem.* **1999**, *38*, 4159−4162. (c) Hay, D. N. T.; Swenson, D. C.; Messerle, L. *Inorg. Chem.* **2002**, *41*, 4700−4747. (d) Basic, I.; Brnicevic, N.; Beck, U.; Simon, A.; McCarley, R. E. *Z. Anorg. Allg. Chem.* **1998**, *624*, 725−732.
(25) Oliaro, F.; Cordier, S.; Halet, J.-F.; Perrin, C.; Saillard, J.-Y.; Sergent, M. *Inorg. Chem.* **1998**, *37*, 6199−6207.
(26) Shen, X. P.; Li, B. L.; Zou, J. Z.; Xu, Z. *Transition Met. Chem.* **2002**, *27*, 372−376.
(27) Scheele, C.-W. *Chemical Essays*; Dawsons of Pall Mall: London, 1786.
(28) Spek, A. L. *PLATON*, version 1.62; University of Utrecht: Utrecht, The Netherlands, 1999.
(29) Breck, D. W. *Zeolite Molecular Sieves*; Wiley & Sons: New York, 1974.
(30) (a) Chen, Z. N.; Wang, J. L.; Qiu, J.; Miao, F. M.; Tang, W. X. *Inorg. Chem.* **1995**, *34*, 2255−2257. (b) Shyu, H. L.; Wei, H. H.; Wang, Y. *Inorg. Chim. Acta* **1997**, *258*, 81−86. (c) Kou, H. Z.; Wang, H. M.; Liao, D. Z.; Cheng, P.; Jiang, Z. H.; Yan, S. P.; Huang, X. Y.; Wang, G. L. *Aust. J. Chem.* **1998**, *51*, 661−666. (d) Zou, J. H.; Xu, X. Y.; Xu, Z.; You, X. Z.; Huang, X. Y.; Zhang, W. L.; Shen, X. P.; Yu, Y. P. *J. Coord. Chem.* **1998**, *43*, 273−280. (e) Mondal, N.; Saha, M. K.; Mitra, S.; Gramlich, V.; Fallah, M. S. E. *Polyhedron* **2000**, *19*, 1935−1939.
(31) (a) Branzea, D. G.; Guerri, A.; Fabelo, O.; Ruiz-Pérez, C.; Chamoreau, L.; Sangregorio, C.; Caneschi, A.; Andruh, M. *Cryst. Growth Des.* **2008**, *8*, 941−949. (b) Zhan, S. Z.; Sun, D. S.; Wang, J. G.; Zhou, J. Y.; Liang, A. Q.; Su, J. Y. *J. Coord. Chem.* **2008**, *61*, 550−562. (c) Akitsu, T.; Einaga, Y. *Inorg. Chem.* **2006**, *45*, 9826−9833. (d) Jiang, L.; Lu, T. B.; Feng, X. L. *Inorg. Chem.* **2005**, *44*, 7056−7062. (e) Colacio, E.; Lloret, F.; Navarrete, M.; Romerosa, A.; Stoeckli-Evans, H.; Suarez-Varela, J. *New J. Chem.* **2005**, *29*, 1189−1194. (f) Berseth, P. A.; Sokol, J. J.; Shores, M. P.; Heinrich, J. L.; Long, J. R. *J. Am. Chem. Soc.* **2000**, *122*, 9655−9662.
(32) (a) Choi, H. J.; Sokol, J. J.; Long, J. R. *J. Phys. Chem. Solids* **2004**, *65*, 839−844. (b) Weihe, H.; Gudel, H. U. *Comments Inorg. Chem.*

DOI: 10.1021/ic502401n
Inorg. Chem. 2015, 54, 1082−1090

2000, *22*, 75−103. (c) Entley, W. R.; Treadway, C. R.; Girolami, G. S. *Mol. Cryst. Liq. Cryst.* **1995**, *273*, 153−166. (d) Glaser, T.; Heidemeier, M.; Weyhermuller, T.; Hoffmann, R.; Rupp, H.; Muller, P. *Angew. Chem., Int. Ed.* **2006**, *45*, 6033−6037.

DOI: 10.1021/ic502401n
Inorg. Chem. 2015, 54, 1082−1090